

PHOTON STRUCTURE

STEFAN SÖLDNER-REMBOLD

CERN, CH-1211 Geneva 23, Switzerland

E-mail: stefan.soldner-rembold@cern.ch

The LEP experiments measure the QED and QCD structure of the photon in deep-inelastic electron-photon scattering. The status of these measurements is discussed in this short review.

1 Kinematics

At LEP the virtuality of the “probing” photon is $Q^2 = -q^2$ (the negative squared four-momentum of the photon) and the virtuality of the “probed” photon is $P^2 = -p^2 \approx 0$. The deep-inelastic scattering cross-section is written as

$$\frac{d^2\sigma_{e\gamma \rightarrow e + \text{hadrons}}}{dx dQ^2} = \frac{2\pi\alpha^2}{x Q^4} \left[(1 + (1-y)^2) F_2^\gamma(x, Q^2) - y^2 F_L^\gamma(x, Q^2) \right], \quad (1)$$

where α is the fine structure constant, x and y are the usual dimensionless variables of deep-inelastic scattering and $W^2 = (q + p)^2$ is the squared invariant mass of the hadronic final state. The scaling variable x is given by

$$x = \frac{Q^2}{Q^2 + W^2 + P^2}. \quad (2)$$

The term proportional to $F_L^\gamma(x, Q^2)$ is small and is therefore usually neglected. In leading order the structure function $F_2^\gamma(x, Q^2)$ can be identified with the sum over the parton densities of the photon weighted by the square of the parton’s charge.

2 QED Structure Functions

The QED structure function F_2^γ has been measured in the process $e^+e^- \rightarrow e^+e^- \mu^+\mu^-$. In addition, the measurement of the distribution of the azimuthal angle χ between the electron scattering plane and the plane containing the muon pair in the $\gamma^*\gamma$ centre-of-mass system gives access to the structure functions F_A^γ and F_B^γ . They are related to the transverse-longitudinal (A) and

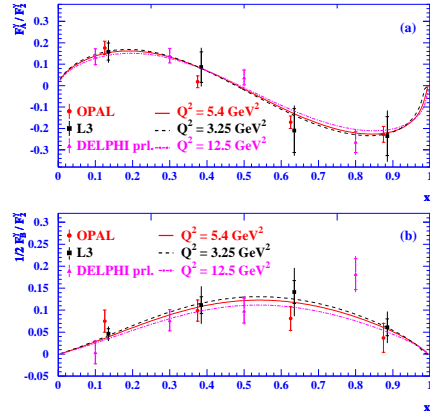


Figure 1. The measured ratios F_A^γ/F_2^γ and $1/2 \cdot F_B^\gamma/F_2^\gamma$ compared to the QED prediction ¹.

the transverse-transverse (B) interference in the interaction of the transverse real photon with the virtual photon. The LEP measurements ^{2,3,4} are shown in Fig. 1. Both structure functions are found to be significantly different from zero and the ratios are well described by QED ¹.

3 Hadronic Structure Functions

The measurement of hadronic structure functions is considerably more difficult due to the necessity to reconstruct x from the hadronic final state in the detector (Eq. 2). Significant progress has been made recently in reducing the systematic errors due to unfolding and hadronisation uncertainties. ALEPH, L3 and OPAL have compared their combined data to the PHOJET and HERWIG generators ⁵.

An unbiased tune using informations from HERA has improved HERWIG significantly.

Furthermore new methods for regularised unfolding like the maximum entropy method or the singular value decomposition method have been used. ALEPH and OPAL have introduced two-dimensional unfolding and improved treatment of hadronic energy in the forward region. L3 is applying energy-momentum conservation using kinematic information from both hadrons and the electrons. The uncertainty on the measurements

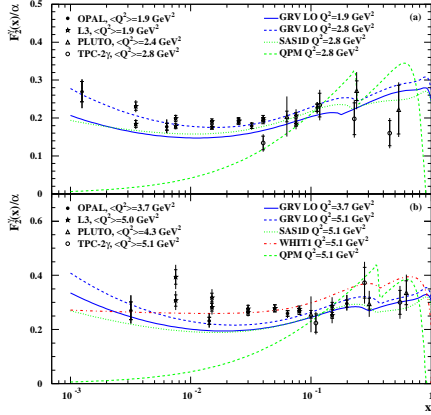


Figure 2. The measured hadronic structure function F_2^γ compared to the GRV-LO⁸, SaS-1D⁹ and the WHIT1¹⁰ parametrisations and to the QPM model. In the case of L3 the values obtained using PHOJET and TWOGLAM for unfolding are shown separately.

shown in Fig. 2 are therefore considerably reduced^{6,7}.

The hadron-like component dominates at low x and there could be a first indication of the low x rise of the photon structure function expected from QCD evolution.

The Q^2 dependence of the structure function F_2^γ in bins of x is shown in Fig. 3 for all currently available measurements. The data are compared to the GRV-HO and the SaS-1D parametrisation, and to the sum of the asymptotic prediction¹¹ for 3 light flavours and the point-like part of the charm structure function taken from GRV. Positive scaling violation of the photon structure function

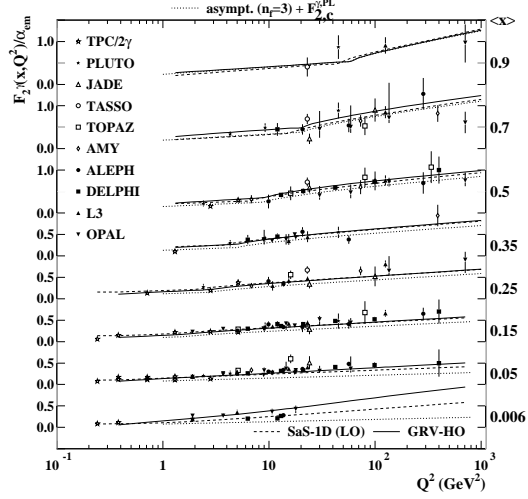


Figure 3. The Q^2 dependence of the hadronic structure function F_2^γ in bins of x compared to the GRV-HO, SaS-1D and the asymptotic prediction.

is observed in all x ranges - different from the proton - due to the regular QCD evolution at low x and due to the inhomogeneous term ($\gamma \rightarrow q\bar{q}$) at larger x . As expected, the asymptotic prediction fails to describe the data at low x , where the non-perturbative hadron-like contribution dominates, whereas all models give a reasonable description of the medium to high x, Q^2 region.

4 Charm Structure Function

In Fig. 3 the charm threshold is clearly visible. Above the kinematic threshold for charm production, the c and u contribution to the point-like part of the photon structure function are of similar size. OPAL has measured the charm structure function of the photon for the first time using D^* decays¹². The region $x > 0.1$ - which is dominated by the point-like component - is in good agreement with a NLO calculation¹³. In the region $x < 0.1$ the measurement suggests the existence of a hadron-like component with currently large errors. These uncertainties are expected to be significantly reduced in the future due to higher statistics and better MC

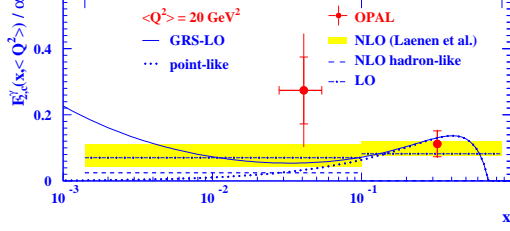


Figure 4. Charm structure function $F_{2,c}^\gamma$ of the photon as function of x for $\langle Q^2 \rangle = 20 \text{ GeV}^2$.

modelling of charm production.

5 Virtual Photon Structure

In addition to the structure function of (quasi-)real photons, i.e. $P^2 \approx 0$, the effective structure function of virtual photons can be measured if $Q^2 \gg P^2 \gg \Lambda_{\text{QCD}}^2$. This was first done by PLUTO ¹⁴. For real pho-

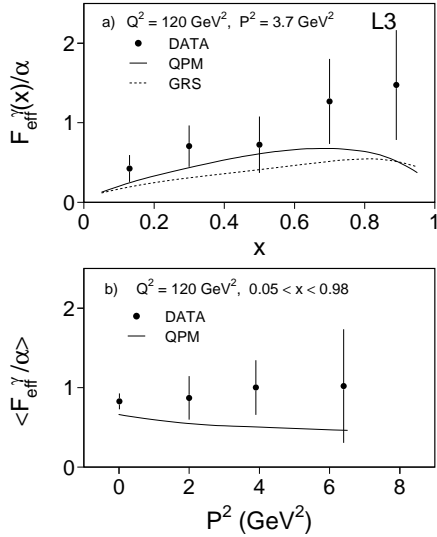


Figure 5. Effective structure function of the virtual photon as function of x and P^2 .

tons only the cross-sections σ_{LT} and σ_{TT} contribute, where the indices refer to the longitudinal and transverse helicity states of the probe and target photon, respectively, i.e. $F_2^\gamma \simeq \sigma_{\text{LT}} + \sigma_{\text{TT}}$. For $P^2 \gg 0$ other helicity states have to be taken into account,

leading to the definition of the effective structure function $F_{\text{eff}}^\gamma \simeq \sigma_{\text{LT}} + \sigma_{\text{TT}} + \sigma_{\text{TL}} + \sigma_{\text{LL}}$ (interference terms are neglected). This effective structure function measured by L3 ¹⁵ is shown in Fig. 5. We expect the hadron-like part of the parton densities at low x to decrease with increasing virtuality of the photon. In Fig. 5b the QPM approximation of the point-like part therefore fails to describe the data point at $P^2 = 0$. The shape of the P^2 dependence is consistent with the QPM ansatz but the errors are still large. Much more precise data is to be expected from LEP on virtual photon structure in the next years.

References

1. R. Nisius, Phys. Rept. 332 (2000) 165.
2. DELPHI note 2000-135, abstract 644 submitted to this conference.
3. L3 Coll., Phys. Lett. B438 (1998) 363.
4. OPAL Coll., Eur. Phys. J. C11 (1999) 409.
5. ALEPH, L3 and OPAL Coll., CERN-EP-2000-109.
6. L3 Coll., Phys. Lett. B447 (1999) 147; Phys. Lett. B436 (1998) 403.
7. OPAL Coll., hep-ex/0007018.
8. M. Glück et al., Phys. Rev. D46 (1992) 1973; Phys. Rev. D45 (1992) 3986.
9. G.A. Schuler et al., Z. Phys. C68 (1995) 607.
10. K. Hagiwara et al., Phys. Rev. D51 (1995) 3197.
11. E. Witten, Nucl. Phys. B120 (1977) 189; in the parametrisation of L.E. Gordon et al., Z. Phys. C56 (1992) 307.
12. OPAL Coll., hep-ex/9911030, see also A. Böhrer, hep-ph/0009121, these proceedings.
13. E. Laenen et al., Phys. Rev. D49 (1994) 5753; E. Laenen, S. Riemersma, Phys. Lett. B376 (1996) 169.
14. PLUTO Coll., C. Berger et al., Phys. Lett. B142 (1984) 119.
15. L3 Coll., Phys. Lett. B483 (2000) 373.